Istraživanja i projektovanja za privredu
ISSN 1451-4117
DOI:10.5937/jaes0-54527
www.engineeringscience.rs

iipp publishing

Journal of Applied Engineering Science
Vol. 23, No. 1, 2025
Original Scientific Paper
Paper number: 23(2025)1, 1260, 141-150

AIR VELOCITY AND PRESSURE MEASUREMENTS OF PORTABLE AIR PURIFIERS USING NUMERICAL SIMULATIONS BASED ON PRODUCT COMPONENT DESIGN VARIATION

Bambang Iskandriawan[1]*, Ahmat Safaat[2] , Bambang Tristiyono[3]

[1] Institut Teknologi Sepuluh Nopember, Centre of Excellence for Creative Design, Faculty of Creative Design and Digital Business, Department of Industrial Design, Surabaya, Indonesia
[2] Institut Teknologi Sepuluh Nopember, Faculty of Vocational, Department of Industrial Mechanical Engineering, Surabaya, Indonesia
[3] Institut Teknologi Sepuluh Nopember, Faculty of Creative Design and Digital Business, Department of Industrial Design, Surabaya, Indonesia
** bisk@its.ac.id*

It is of great importance to ascertain the airflow pattern around a device that functions by blowing out air, as the resulting airflow pattern will ultimately determine the device's performance. The airflow pattern surrounding an air purifier is greatly influenced by the product design of its constituent components, especially the blow air diffuser and the return air components. Given the growing and, to some extent, compulsory usage of portable air purifiers among the general public, especially among those concerned with maintaining good indoor air quality, this study aimed to identify the optimal product component design for portable air purifiers. This was achieved by considering the effects of air velocity and pressure on the performance of the air purifiers. In this study, a numerical simulation application was employed to obtain data on air velocity and pressure for each product component design variation. The objective was to generate a report on air velocity and pressure for various component design variations of high-efficiency particulate air (HEPA) filters, including variations in height and diameter, rotor blade tilt angle and width, and inlet hole casing design pattern.

Keywords: air velocity and pressure measurements, portable air purifier, numerical simulations, product component design variations, airflow pattern

1 INTRODUCTION

The use of air purifiers has become increasingly common, especially during the COVID-19 pandemic. Typically, air purifiers are used in regions prone to frequent forest or land fires. Air purifiers are also often utilized in indoor spaces with a considerable number of occupants, such as classrooms, places of worship, and meeting rooms. The rationale behind the use of an air purifier is that the device can effectively remove pollutants from the air, thereby reducing the risk of exposure to contaminated air by the individuals within the room. An investigation has successfully demonstrated the efficacy of air filters in improving the quality of indoor air by reducing the concentration of air pollution, although it has been acknowledged that a definitive link between this improvement and health outcomes has yet to be established [1]. Regarding this topic, the efficacy of an air filter in reducing fine particles suspended in the air is very dependent on the air velocity characteristics generated by the device [2]. A deficiency in air velocity will have no impact on the reduction of air pollutant concentrations. Two important factors, namely the location of installation and the number of air purifiers operated in temporary plastic anterooms, have been investigated [3]. Optimizing the number and placement of air purifies in isolation and anterooms in hospitals is an intriguing topic of discussion. The relationship between user perception and air purifier design elements, such as facade, cross-section, switch adjustment, color, and material, has been discussed [4].

The investigation was accomplished to quantitatively assess the effect of air purifiers on the spread of COVID-19 and to recommend procedures for their safe and effective application. The dispersion of simulated respiratory droplet nuclei by the air purifier was found to be inconsequential, but nano-aggregates were considerably disrupted by the airflow generated by the air purifier. However, because of the high-efficiency particulate air (HEPA) filter within the air purifier, which effectively eliminates airborne particles, the incessant operation of the air purifier resulted in a notable reduction in the concentration of both simulated respiratory droplet nuclei and nano-aggregates, in comparison to the trial that did not include air purifier control [5]. Throughout the operational day, thermal comfort was reasonably acceptable, with an insignificant escalation in indoor temperature standards for particular cases and the majority of relative humidity values remaining within the recommendation limits. The use of CO_2 as an indicator of the clinic ventilation level led to the conclusion that the mechanical ventilation system was capable of maintaining tolerable levels of indoor air quality even when the clinic was in use by a large number of people. The measured total volatile organic compounds (TVOC) levels were found to be relatively low, despite the frequent use of dental materials within the clinic during the designated work shift, which resulted in many instances of maximum concentration. The concentration of particulate matter with a diameter of 2.5 μm or less (PM2.5) and with a diameter of 10 μm or less (PM10) exhibited a notable decrease throughout the experimental period, with a

few exceptions, mainly attributable to episodes of external atmospheric pollution [6]. The operation of portable air purifiers has been observed to yield a discernible benefit, particularly in the reduction of viral concentrations [7].

The results of the constraint study, conducted using the computation pattern, indicated that the parameters with the greatest influence on the latent dose of virus-loaded particles were the dimensions of the area, the duration of stay, and the movement of people within the room. The use of central air conditioning systems has been demonstrated to be an ineffective method for the elimination of particles discharged from virulent mouths, with the majority of the particles being dispersed throughout the room and ultimately deposited on inhabitants, furniture, equipment, the floor, and partitions [8]. Similarly, both floor-standing and tabletop air purifiers, positioned and sized correctly, can excellently draw room air into the purifier and subsequently produce uncontaminated air. The valuation of air conditioning and the degree of its decontamination should consider the physical qualities of temperature, humidity, CO_2, and particulate matter (PM). However, it is of greater importance to consider biological facts. The objective of air purification in schools has been the subject of considerable research, intending to develop tools that do not increase the microbiological and PM quality of the air [9]. It is important to note that the real efficacy of air purifiers may vary considerably from that stated by industrialists. The precise selection of the device, which is specific to each classroom, serves a main function. Before operating devices for air purification in large-volume and high-density rooms, it is advisable to ascertain their efficacy on-site, as the cleaning efficiency is constrained by the manufacturer for less than optimal medical rooms and a small number of individuals. The deployment of air purifiers in school classrooms was observed to reduce PM intensities by approximately 30%, a level that falls below the Indoor Air Quality (IAQ) standard [10]. However, CO_2 concentrations in the majority of classrooms exceeded 1000 ppm, indicating insufficient ventilation and that PM and CO_2 should be controlled instantaneously. The impact levels of indoor PM sources in elementary, middle, and high schools were greater than those of outdoor sources. The type of surface materials, the presence of play area materials, and the existence of shoe cupboards had a considerable influence on the concentration of PM in classrooms.

Notably, the scientific journal articles on the topic of air filters, as previously mentioned, do not specifically address the air velocity flow and pressure drop exiting air purifiers concerning the design of portable air purifier components. The autonomy of air purifier designers to develop their creativity is certainly constrained by the findings of this research. Numerical simulation programs are invaluable for researchers seeking to analyze both the airflow around a product and the structure of a product design that has been created by [11], [12], [13], [14] and [15]. Nevertheless, the findings may serve as a guide for designers and practitioners in the development of more beneficial and aesthetically pleasing related products. The numerical simulation results have served to reinforce the findings of the investigative process. Two distinct ventilated blade designs were employed: the SC rotor and the SV05 model. The results demonstrated that ventilation with a 5% gap width of the blade diameter (SV05 model) exhibited the greatest static torque. This approach has the potential to enhance the static torque of a conventional Savonius rotor by up to 23.8% [16]. The model outcomes demonstrate the capacity of numerical simulation in envisaging the flow properties over a series of circular cylinders arranged in equispaced positions along the centerline of the laboratory canal. Three arrangements of cylinders with diameters corresponding to the aforementioned ratios were investigated under uniform flow settings [17]. The inquiry defines the procedure for modeling the reestablishment processes of the demolished sector of the spline and its whole restoration operating modern techniques, such as hard facing in a protective gas environment with a disposable electrode. The numerical simulation software with a supplementary technique extension was employed to simulate the practice of hardfacing a scratched surface. The simulation outcomes were found to be in reliable conformity with the experimental facts [18].

2 MATERIALS AND METHODOLOGIES

Modeling and simulation using software in the form of Solidworks to model geometry in 3 dimensions and Ansys Fluent 2023 R1 for numerical simulation of air purifiers. Each software has a use license in the name of ITS. The model refers to a commercial air purifier, namely the Krisbow Sync 24 M2 Smart Air Purifier with a 1:1 ratio. Some components that do not affect the overall functionality were simplified to prevent errors during the meshing process and simulation execution (Figure 1). The modeling and simulation steps can be seen in Figure 2.

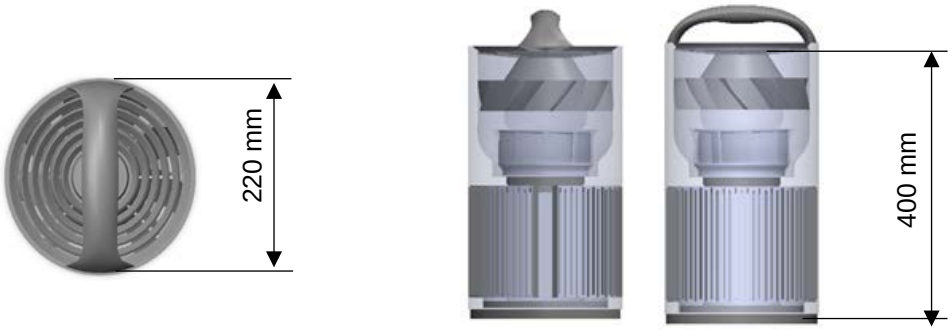

Fig. 1. Three-dimensional (3D) image of a portable air purifier product, which served as a model for a numerical simulation process based on existing commercial products

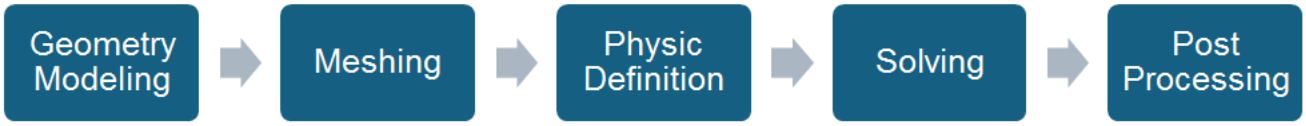

Fig. 2. Stages of the numerical simulation work process to observe the outlet air velocity and pressure around the air purifier product

Steps in modeling and simulation can be explained as follows:

1. Geometry modeling: the air purifier is dismantled starting from the casing/cover, rotor, stator, HEPA filter, and other components. Each component is measured as material for making a model/geometry in 3D software (Solidworks).
2. The meshing stage is carried out to divide the geometry into small elements for the calculation process in the simulation.
3. Physical definition: the definition of the geometries involved in the simulation is determined, the definition of geometry includes loading, constraints, and environmental conditions.
4. Solving: based on geometry, meshing, and physical definition, a mathematical model/equation for the case raised is obtained. In this process, calculations/completion of the equations that apply to the model are carried out.
5. Post Processing: after carrying out calculations, the results are obtained in the form of outlet air velocity and pressure acting on the control volume.

Figure 3 illustrates the boundary conditions that apply to the air purifier simulation, as follows:

a) The control volume is defined as an air-fluid;
b) The top surface is defined as a pressure outlet;
c) The side surface is defined as a pressure outlet;
d) The bottom surface is defined as the wall;
e) The air purifier body, static blade, and blade on the rotating part are defined as the wall;
f) The outer side of the rotating component is defined as air-to-air contact;
g) The filter is defined as the porous zone;
h) No transfer of heat or generation of energy occurs;
i) The fan rotates at a rate of 1500 rpm.

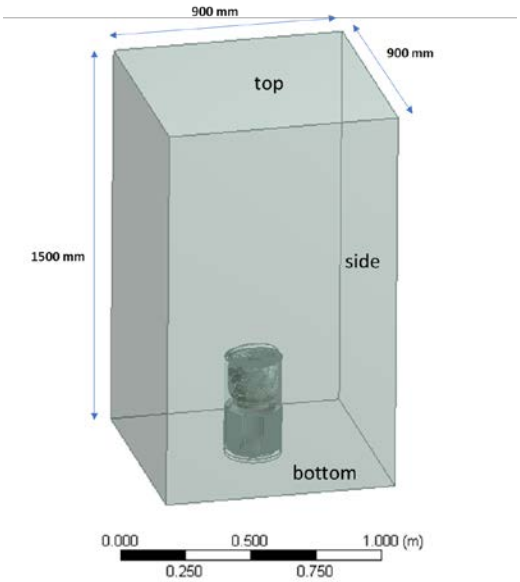

Fig. 3. Boundary condition dimension on the numerical simulation of the air purifier product

The Navier-Stokes equation is used as a mathematical model in the simulation (Equation 1) [19].

$$\rho \frac{D\vec{V}}{Dt} = -\vec{\nabla}P + \rho\vec{g} + \mu\nabla^2\vec{V} \quad (1)$$

To solve fluid flow problems, it is needed both the continuity equation and the Navier-Stokes equation. Since it is a vector equation, the Navier-Stokes (NS) equation is usually split into three components to solve fluid flow problems. Incompressible continuity equation in cartesian coordinates (Equation 2).

$$\frac{\partial u}{\partial x}+\frac{\partial v}{\partial y}+\frac{\partial w}{\partial z}=0 \quad (2)$$

The x, y, and z components of the incompressible NS equation (Equations 3, 4, and 5).

$$\rho\left(\frac{\partial u}{\partial t}+u\frac{\partial u}{\partial x}+v\frac{\partial u}{\partial y}+w\frac{\partial u}{\partial z}\right)=-\frac{\partial P}{\partial x}+\rho g_x+\mu\left(\frac{\partial^2 u}{\partial x^2}+\frac{\partial^2 u}{\partial y^2}+\frac{\partial^2 u}{\partial z^2}\right) \quad (3)$$

$$\rho\left(\frac{\partial v}{\partial t}+u\frac{\partial v}{\partial x}+v\frac{\partial v}{\partial y}+w\frac{\partial v}{\partial z}\right)=-\frac{\partial P}{\partial y}+\rho g_y+\mu\left(\frac{\partial^2 v}{\partial x^2}+\frac{\partial^2 v}{\partial y^2}+\frac{\partial^2 v}{\partial z^2}\right) \quad (4)$$

$$\rho\left(\frac{\partial w}{\partial t}+u\frac{\partial w}{\partial x}+v\frac{wv}{\partial y}+w\frac{\partial w}{\partial z}\right)=-\frac{\partial P}{\partial z}+\rho g_z+\mu\left(\frac{\partial^2 w}{\partial x^2}+\frac{\partial^2 w}{\partial y^2}+\frac{\partial^2 w}{\partial z^2}\right) \quad (5)$$

The results obtained are in the air velocity and pressure values at each point which have been determined as could be seen in Figure 4. This discussion is limited to the y-axis area only (height position).

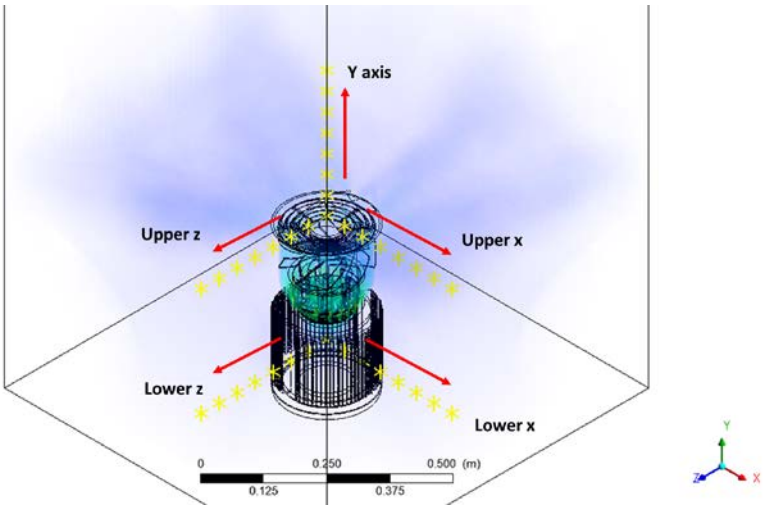

Fig. 4. Measurement points of air velocity and pressure around the air purifier model.

2.1 HEPA filter height variation

Figure 5 illustrates four distinct variations in HEPA filter height dimensions. The height of the HEPA filter (h_H) in the commercially available air purifier product was 158 mm. It can be observed that as the HEPA filter became shorter, the total height of the air purifier unit decreased.

A B C D

Fig. 5. The design of the HEPA filter with four variations in height, designated as h_H: 158, 118.5, 79.0, and 39.5 mm, respectively

2.2 HEPA filter diameter variation

Five variations in HEPA filter diameter lengths were established. The diameter of the HEPA filter in the commercially available air purifier product, designated as D_H, was 111 mm. As the diameter of the HEPA filter decreased, the gap formed between the HEPA filter and the lower casing of the air purifier increased (Figure 6). In this case, the diameter of the air purifier was fixed.

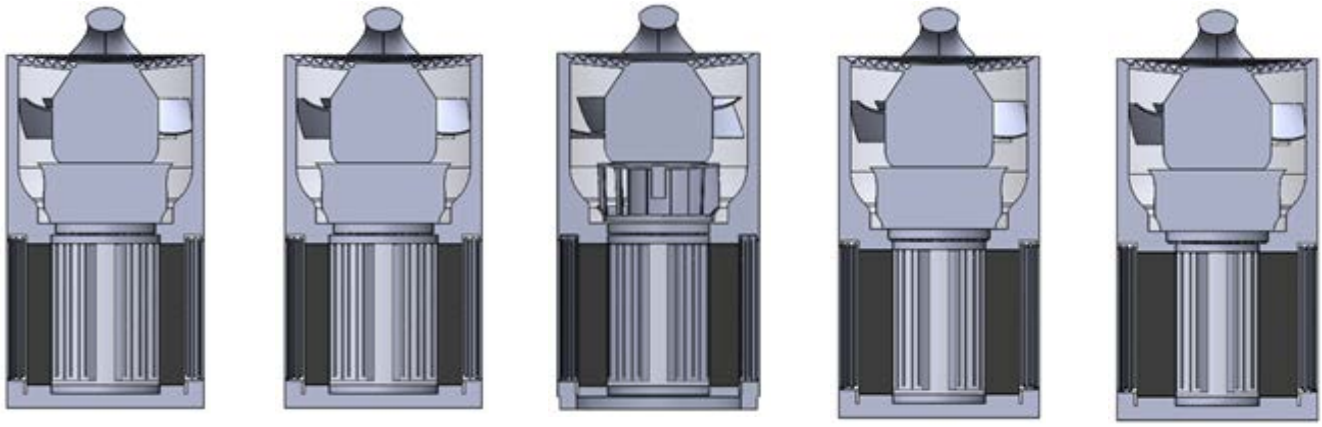

Fig. 6. The design of the HEPA filter components with five variations of diameter (D_H): 131, 121, 111, 101, and 91 mm, respectively

2.3 Rotor blade tilt angle variation

Five variations of rotor blade angle inclination were determined, as illustrated in Figure 7. The tilt angle of the rotor blade in the commercially available air purifier (α_{RB}) was determined to be 55º. It is postulated that the rotor blade tilt angle may influence the smoothness of airflow within the internal air purifier.

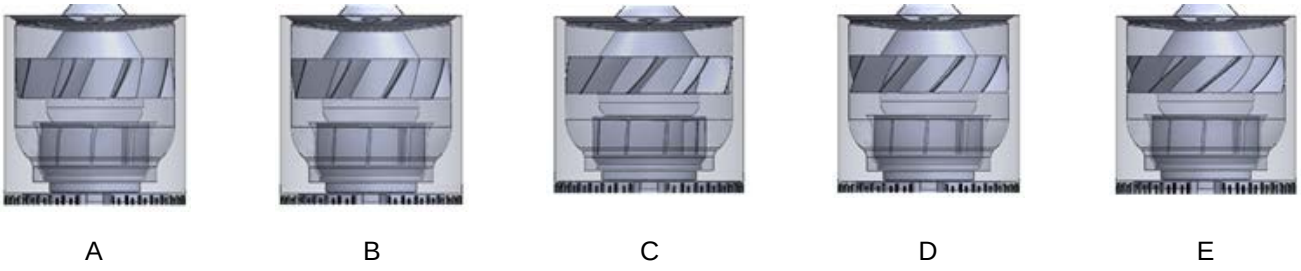

Fig. 7. Rotor blade component designs with five variations of tilt angle, α_{RB}: 65º, 60º, 55º, 50º, and 45º

2.4 Rotor blade width variation

Four variations in rotor blade width were set, with the width of the rotor blade (w_{RB}) in the commercially available air purifier product being 41 mm. As the width of the rotor blade decreased, the gap formed between the rotor and the air purifier casing tended to become slighter (Figure 8). In this case, the diameter of the air purifier diameter remained constant.

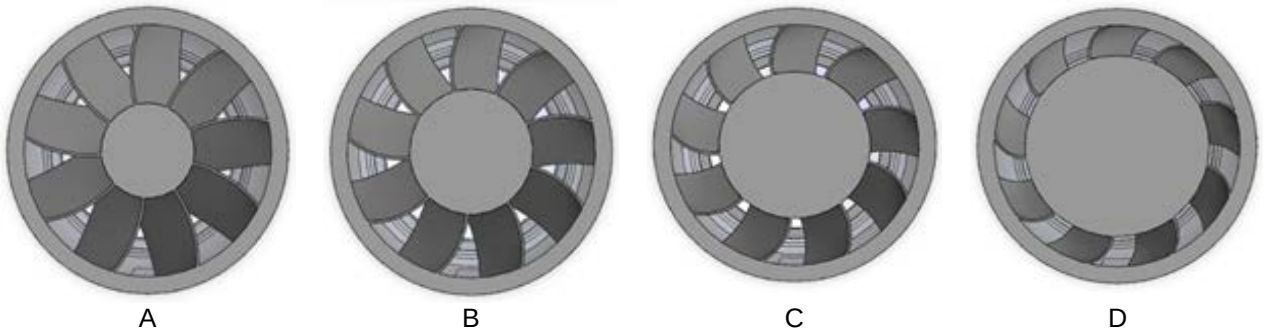

Fig. 8. Designs of rotor blade components with four variations of width (w_{RB}): 61, 51, 41, and 31 mm

2.5 Inlet casing design pattern variation

Five variations in the casing hole component of the air purifier for return air were concluded (Figure 9). The design of the commercially available air purifier product was found to be similar to A.

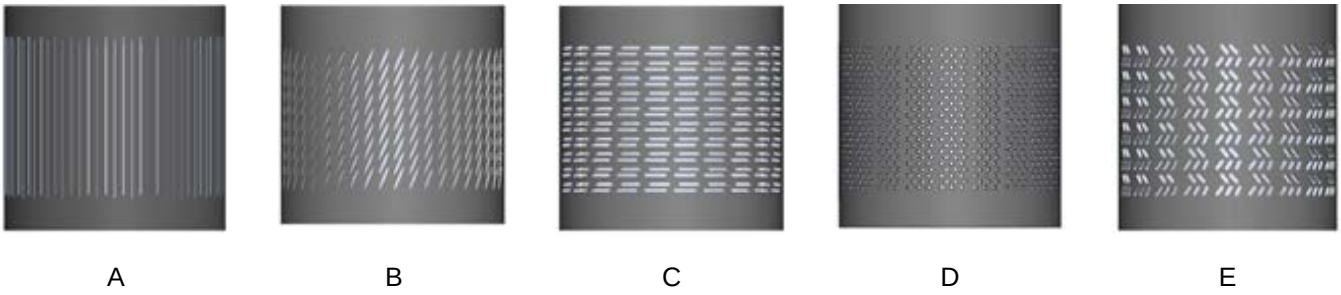

Fig. 9. Inlet casing hole components with five variations in design pattern

3 RESULTS AND DISCUSSION

3.1 HEPA filter height

The most important component of the air purifier device is the HEPA filter. The height (h_H) of the HEPA filter in the commercially available air purifier product was 158.0 mm. As illustrated in Figure 10, a reduction in the height of the HEPA filter resulted in a corresponding decrease in outlet air velocity. A reduction in the suction area is tantamount to a reduction in the volume of air drawn. Except for certain areas between the heights (h) of 400 mm to approximately 480 mm, the air velocity of the HEPA filter at a height (h_H) of 158.0 mm was observed lower than that of the height (h_H) of 118.5 mm. In general, a reduction in the height (H) of the HEPA filter by 25% resulted in a decrease in outlet air velocity (V_{out}) by 0.7%. For a 50% reduction in H, V_{out} was reduced by 18.1%, and for a 75% reduction in H, V_{out} was reduced by 44.7%. The highest outlet air velocity (V_{out}) for each HEPA filter height (h_H) was observed in the area around a height (h) of 500 mm. At the initial height position, the pressures are different; as the HEPA filter height decreased, the outlet air pressure increased. However, in most cases, the direction of the airflow was upward, resulting in a pressure gradient toward the same point.

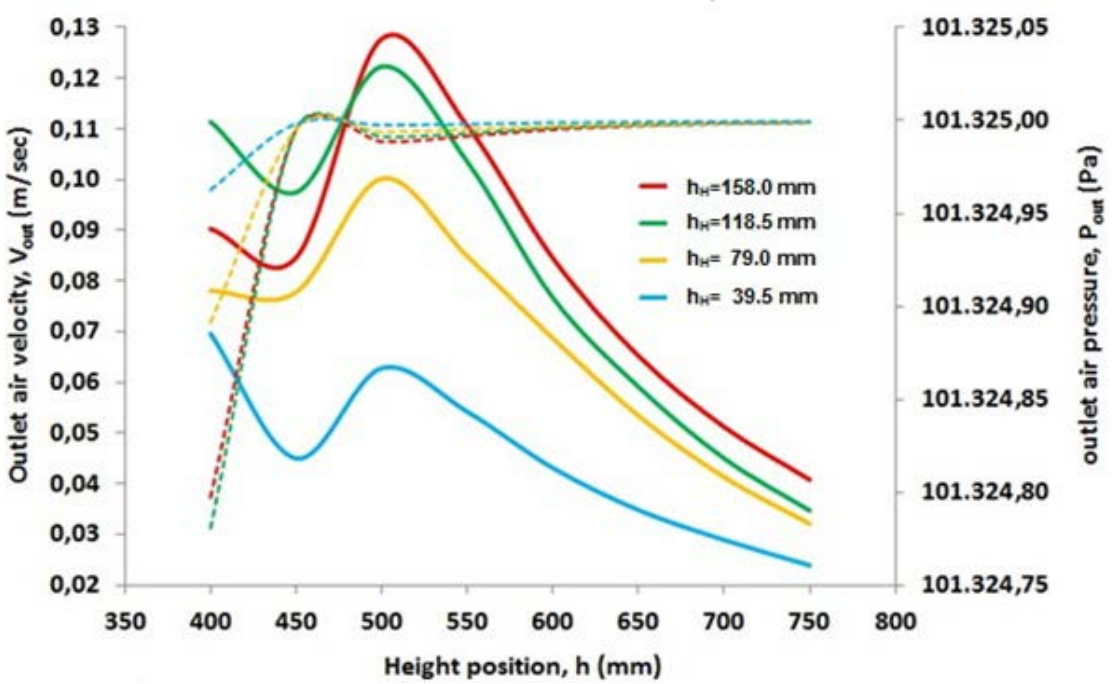

Fig. 10. Outlet air velocity (full lines) and pressure (dashed lines) around the air purifier unit with four variations in the height (h_H) of the HEPA filter component: 158.0, 118.5, 79.0, and 39.5 mm

3.2 HEPA filter diameter

The commercial air purifiers utilized HEPA filters with a diameter (D_H) of 111 mm. Figure 11 shows that a reduction in the diameter of the HEPA filter resulted in a corresponding decrease in outlet air velocity, and vice versa. A reduction of the suction area is tantamount to a reduction in the volume of air sucked in. Except for certain areas, particularly those situated between heights (h) of 400 mm and approximately 450 mm, the airflow rate remained irregular. In typical circumstances, a reduction in the diameter of the HEPA filter (D_H) by 18% resulted in a decrease in outlet air velocity (V_{out}) by 1.3 %, while an increase in D_H by the same amount led to an amplification of V_{out} by 17.3%. It is noteworthy that a reduction in the diameter of the HEPA filter by 9% resulted in a 34.7% increase in the outlet air velocity (V_{out}) for a filter with a diameter (D_H) of 101 mm. Therefore, in this case, the optimal HEPA filter diameter (D_H) was 101 mm. At the initial height position, the pressures are different; as the

HEPA filter diameter increased, the outlet air pressure decreased. However, in many cases, the direction of the airflow was upward, resulting in the pressure approaching the same point.

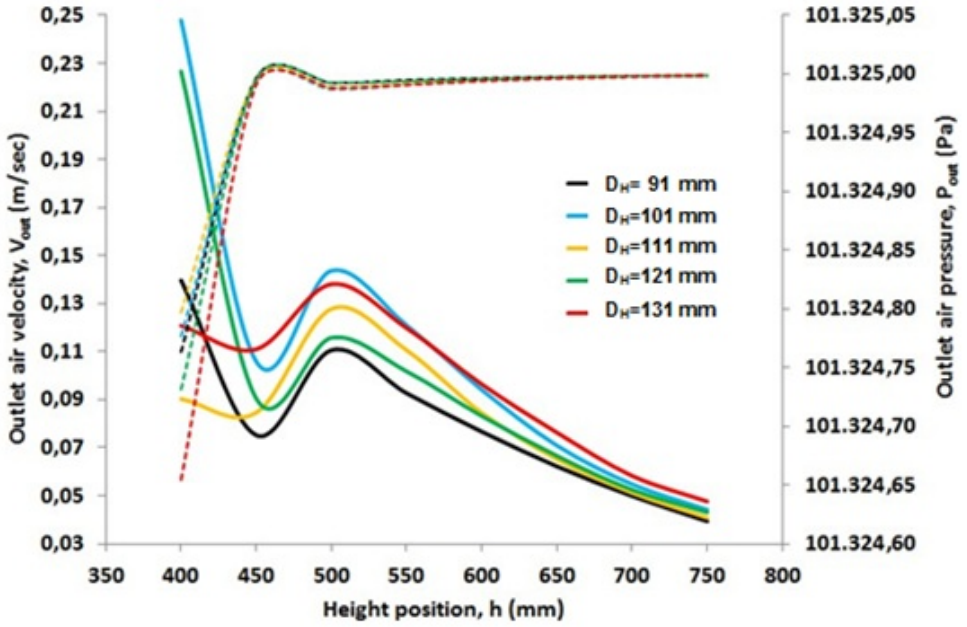

Fig. 11. Outlet air velocity (full lines) and pressure (dashed lines) around the air purifier unit with five variations in the diameter (D_H) of the HEPA filter component: 91, 101, 111, 121, and 131 mm

3.3 Blade tilt angle

Another important component of an air purifier unit is the rotor component, which is responsible for regulating the airflow in and out of the unit. The blade tilt angle of the commercial air purifier was α_{RB} = 55º. As illustrated in Figure 12, an increase in the blade tilt angle resulted in a drop in outlet air velocity. Conversely, a reduction in blade tilt angle increased outlet air velocity. Overall, a reduction in the blade tilt angle of the rotor, α_{RB}, by 18.2 % resulted in an increase in outlet air velocity, V_{out}, by 41.2%. Conversely, an increase in α_{RB} by 18.2 % led to a decrease in V_{out} by 35.2 %. At the initial height position, the pressures were different but often with the direction of the air coming out upwards, the amount of pressure was toward the same point.

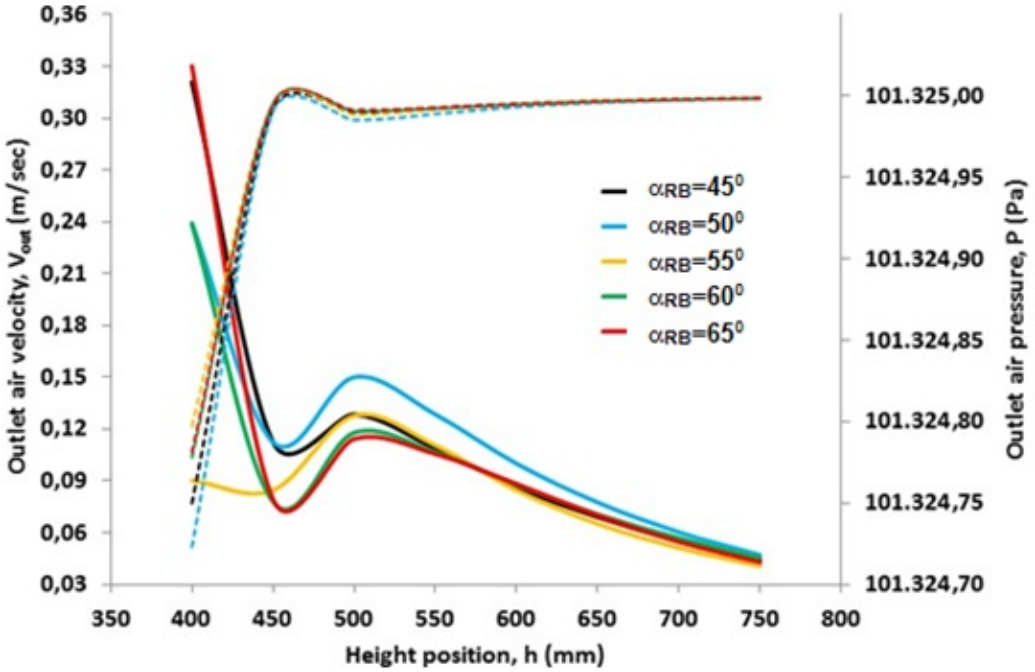

Fig. 12. Outlet air velocity (full lines) and pressure (dashed lines) around the air purifier unit with five variations of rotor component blade tilt angle (α_{RB}): 45º, 50º, 55º, 60º, and 65º

3.4 Rotor blade width

The width of the rotor blades serves to determine the airflow rate of the air purifier unit. The rotor blade width (w_{RB}) of the commercially available air purifier was 41 mm. It can be seen from Figure 13 that an increase in rotor blade

width (w_{RB}) of 48.8% and a decrease of 24.4% yielded comparable outcomes in outlet air velocity (V_{out}), namely a decrease of approximately 1.3% for height positions (h) between 450 and 750 mm. An increase in blade width of 24.4% resulted in the two-outlet air velocity (V_{out}) graphs coinciding. This indicates that the increase in blade width is insufficient to produce a significant effect. At the initial height position, the pressures were disparate, but often with the direction of the air coming out upwards, the magnitude of pressure was toward the identical point.

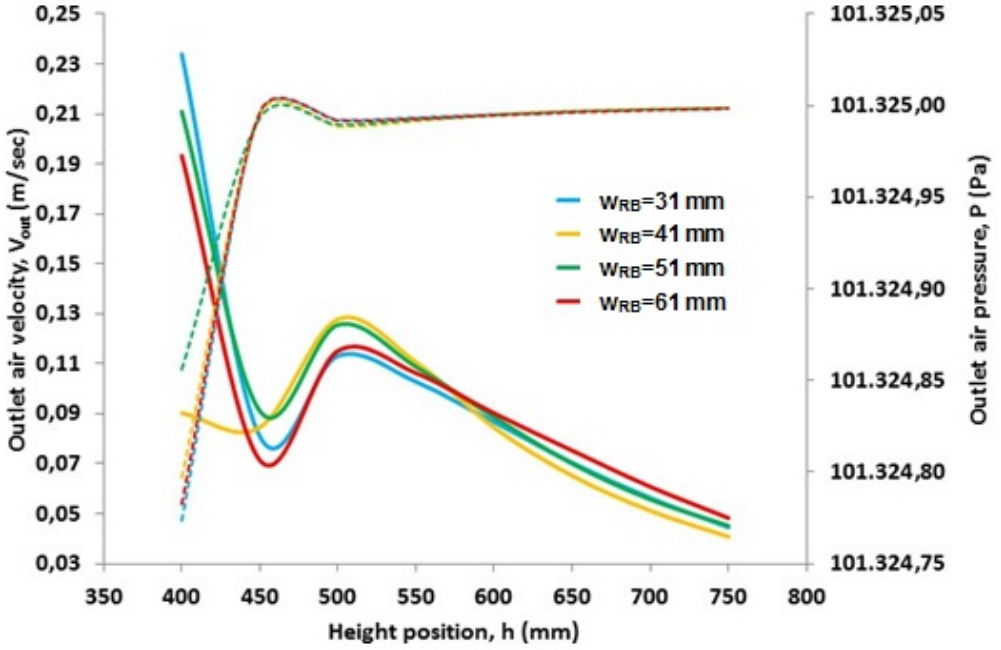

Fig. 13. Outlet air velocity (full lines) and pressure (dashed lines) around the air purifier unit with four variations of rotor blade component width (w_{RB}): 31, 41, 51, and 61 mm

3.5 Inlet casing design pattern

There were five variations of inlet casing design patterns, where the design of the commercial air purifier is similar to pattern A (Figure 14). For heights (h) between 400 and 500 mm, the most optimal inlet casing design pattern was C, E, D, B, and A, in that order. Following the height position (h) of 500 mm, the five outlet air velocity graphs almost coincided. A similar trend was observed in the outlet air pressure graphs, which demonstrated remarkable consistency across all height positions (h).

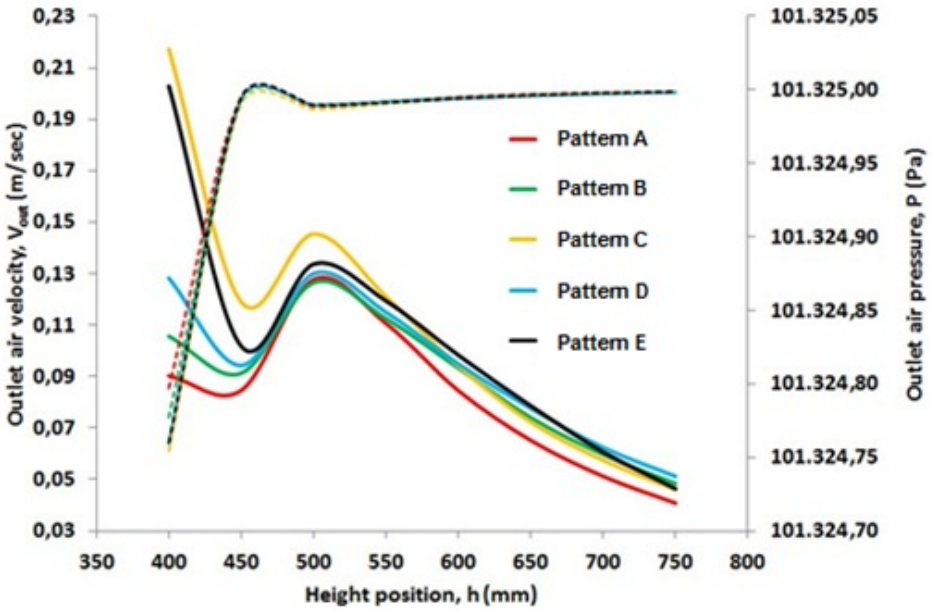

Fig. 14. Outlet air velocity (full lines) and pressure (dashed lines) around the air purifier unit with five inlet casing hole component variations in the design pattern

4 CONCLUSIONS

The influence of HEPA filter height and diameter, blade tilt angle and width, and inlet casing design pattern on the outlet air velocity and air pressure above the air purifier equipment can be concluded based on experiments using

numerical simulation methods. A reduction in HEPA filter height (H_H) will result in a corresponding reduction in outlet air velocity (V_{out}). A HEPA filter height (H_H) of 158 mm has been identified as an optimal filter height. The effect of HEPA filter height (H_H) on outlet air pressure (P) is only discernible at the starting point, after which the pressure remains constant for each HEPA filter height (H_H).

In general, an increase in HEPA filter diameter (D_H) will result in the amplification of outlet air velocity (V_{out}), and vice versa. It should be noted, however, that the increase or decrease in HEPA filter diameter should be significant enough to yield meaningful results. In the case of this study, the decrease or increase was 18%. Interestingly, a small decrease of 9% resulted in a notable increase in outlet air velocity (V_{out}). This investigation has identified that the best HEPA filter diameter (D_H) is 101 mm, based on the five diameter sizes that were tested. The outlet air pressure (P) graph almost coincided with the height position (h) above the air purifier equipment.

The most acceptable blade tilt angle (α_{RB}) was found to be 50º in this assessment, especially for areas above the height position (h) of 450 mm. Notably, the α_{RB} of 45º is even more pronounced but only for the area below the height position (h) of 450 mm.

The rotor blade width (W_{RB}) of 41 mm is optimal, especially for areas above the height position (h) of 450mm. Modifications to the rotor blade width (W_{RB}) will increase the outlet air velocity (V_{out}), but only for the area below the height position (h) of 450 mm.

The experiment investigating the inlet casing design pattern has successfully identified the optimal configuration for achieving the highest outlet air velocity (V_{out}). The superiority of the inlet casing design patterns C and E can be attributed to their higher frequency of holes, which facilitates a more streamlined airflow into the air purifier. However, there is a potential downside to larger holes, namely that they may lead to accelerated dirt accumulation and clogging of the HEPA filter.

5 ACKNOWLEDGMENT

We would like to thank the Directorate of Research and Community Service (DRPM) of Institut Teknologi Sepuluh Nopember (ITS), Surabaya, Indonesia, for providing a flagship fund that enabled the successful completion of this study.

6 REFERENCES

[1] Yoda, Y., Tamura, K., Adachi, S., Otani, N., Nakayama, S.F., Shima, M. (2020). Effects of the use of air purifier on indoor environment and respiratory system among healthy adults. International Journal of Environment Research and Public Health, vol. 17, 3687; doi:10.3390/ijerph17103687.

[2] Park, H., Park, S., Seo, J. (2020). Evaluation of air Purifier's performance in reducing the concentration of fine particulate matter for occupants according to its operation methods. International Journal of Environment Research and Public Health, vol. 17, 5561; doi:10.3390/ijerph17155561.

[3] Mousavi, E.S., Pollitt, K.J.G, Sherman, J., Martinello, R.A. (2020). Performance analysis of Portable HEPA filters and temporary plastic anterooms on the spread of surrogate coronavirus. Building and Environment, vol. 183. 0360-1323/© 2020 Elsevier. http://doi.org/10.1016/j.buildenv.2020.107186.

[4] Wang, M., Cheng, Xufeng, C., Liang, J. (2021). Research on the design of a portable desktop air purifier based on Kansei Engineering. DOI 10.1109/ACCESS.2021.3119203.

[5] Heo, K.J., Park, I., Lee, G., Hong, K., Han, B., Jung, J.H., Kim, S.B. (2021). Effects of air purifiers on the spread of simulated respiratory droplet nuclei and virus aggregates. International Journal of Environmental Research and Public Health, vol. 18, 8426. https://doi.org/10.3390/ijerph18168426.

[6] Tzouttzas, I., Maltezou, H.C., Barmparesos, N., Tasious, P., Efthymiou, C., Assmakopoulos, M.N., Tseroni, M., Vorou, R., Tzermpos, F., Antoniadou, M., Panis, V., Madianos, P. (2021). Indoor air quality evaluation using mechanical ventilation and portable air purifiers in an academic dentistry clinic during the Covid-19 pandemic in Greece, International Journal of Environmental Research and Public Health, vol. 18, 8886. https://doi.org/10.3390/ijerph18168886.

[7] Duill, F.F., Schulz, F., Jain, A., Krieger, L., Wachem, B.V., Beyrau, F. (2021). The impact of large mobile air purifiers on aerosol concentration in classrooms and the reduction of airborne transmission of SAR-CoV-2. International Journal of Environmental Research and Public Health, vol. 18,11523. https://doi.org/10.3390/ijerph182111523.

[8] Zhai, Z (J)., Li, H., Bahl, R., Trace, K. (2021). Application of Portable Air Purifiers for mitigating COVID-19 in large public space. Buildings, vol. 11, 329. http://doi.org/10.3390/buildings11080329.

[9] Basinska, M., Michalkiewicz, M., Ratajczak, K. (2021) Effect of air purifier use in the classrooms on indoor air quality-case study, atmosphere, vol. 12, 1606. http://doi.org/10.3390/atos12121606.

[10] Choe, Y., Shin, J., Park, J., Kim, E., Oh, N., Min, K., Kim, D., Sung, K., Cho, M., Yang, W. (2022). Inadequacy of air purifiers for indoor air quality improvement in classrooms without external ventilation. Building Environment, vol. 207. 0360-1323/© 2021 Elsevier Ltd. https://doi.org/10.1016/j.buildenv.2021.108450.

[11] Iskandriawan, B., Jatmiko, J., Safaat, A., Nugraha, J.A. (2020). Air Velocity and pressure drop exploration inside pipe frame of air purifier bicycle using numerical analysis. *Journal of Engineering Science and Technology*, vol. 15, no. 6, 2935-3954, © School of Engineering, Taylor's University.

[12] Budiyanto, M.A., Naufal, F., Putra, G.L., Riadi, A., Suprayogi, D.T., Iqbal, M., Pribadi, T.W. (2024). Numerical investigation into the pressure and flow velocity distributions of a slender-body catamaran due to viscous interference effects. *International Journal of Technology*, vol 15, no. 2, 247-258

[13] Cicero, S., Lacalle, R., Cicero, R., Fernandez, D., Mendez, D. (2011). Analysis of the cracking causes in aluminum alloy bike frame. *Engineering Failure Analysis,* vol. 18, no. 1, 34-46

[14] Kujawa, M., Lubowiecka, I., Szymczak, C. (2020). Finite element modeling of a historic church structure in the context of masonry damage analysis. *Engineering Failure Analysis,* vol 107, 1-18

[15] Iskandriawan, B. (2023). Structure simulation on portable commuter bike considering frame design and material alternatives. *Journal of Engineering and Technological Sciences*, vol. 55, no. 1, 11-21, DOI.10.5614/j.eng.technol.sci.2023.55.1.2.

[16] Hariyanto, R., Soeparman, S., Widhiyanuriyawan, D., Sasongko, M.N. (2018). CFD study on the ability of a ventilated blade in improving the savonious rotor performance, Journal of Applied Engineering Science, vol. 16, No. 3, 383-390, doi:10.5937/jaes16-17189.

[17] Al-Osmy, S.A.T., Al-Hashimi, S.A.M., Mulahasan, S., Fartosy, S.H. (2023). Simulation of flow through an equispaced in-line cylinder in open channels. Journal of Applied Engineering Science, vol. 21, no.1. 253-262, doi:10.5937/jaes0-40078.

[18] Nurzhanova, O., Zharkevich, O., Bessonov, A., Naboko, Y., Abdugaliyeva., G., Taimanova, G., Nikonova, T. (2023). Simulation of the distribution of temperature, stresses, and deformations during splined shafts hard-facing. Journal of Applied Engineering Science, vol. 21, no. 3, doi: 10.5937/jaes0.42774.

[19] Min, H., Shin, J., Choi, J., Lee, H. (2017). Modeling and simulating flow phenomenon using Navier-Stokes equation. Proceedings of the International Conference on Industrial Engineering and Operations Management, Rabat, Morocco, April 11-13, 2017, p.1902-1912

Paper submitted: 03.11.2024.

Paper accepted: 04.02.2025.